Differential Effects of Glucose and Glyburide on Energetics and Na^+ Levels of βHC9 Cells

Nuclear Magnetic Resonance Spectroscopy and Respirometry Studies

Nicolai M. Doliba,[1] Marko Z. Vatamaniuk,[1] Carol W. Buettger,[1] Wei Qin,[1] Heather W. Collins,[1] Suzanne L. Wehrli,[2] Richard D. Carr,[3] and Franz M. Matschinsky[1]

In the present study, noninvasive ^{31}P and $^{23}Na^+$–nuclear magnetic resonance (NMR) technology and respirometry were used to compare the effect of high glucose (30 mmol/l) with the effect of the antidiabetic sulfonylurea (SU) compound glyburide (GLY) on energy metabolism, Na^+ flux, insulin, and cAMP release of continuously superfused β-HC9 cells encapsulated in microscopic agarose beads. Both high glucose and GLY increased oxygen consumption in β-HC9 cells (15–30%) with a maximal effect at 8 mmol/l for glucose and at 250 nmol/l for GLY. At the same time, insulin release from β-cells increased by 15- and 25-fold with high glucose or GLY, respectively. The P-creatine (PCr) level was greatly increased and inorganic phosphate (P_i) was decreased with 30 mmol/l glucose in contrast to the decreased level of PCr and increased P_i with GLY. ATP levels remained unchanged during both interventions. Studies on isolated mitochondria of β-HC9 cells showed that GLY added to mitochondria oxidizing glutamine or glutamate abolished the stimulation of respiration by ADP (state 3) meanwhile leaving state 3 respiration unchanged during oxidation of other substrates. Exposure of β-HC9 cells to 5 mmol/l glucose decreased intracellular Na^+ levels monitored by $^{23}Na^+$-NMR spectroscopy and 30 mmol/l glucose resulted in a further decrease in cytosolic Na^+. In contrast, Na^+ increased when 1 μmol/l GLY was added to the perfusate containing 5 mmol/l glucose. These data support the hypothesis that glucose activates the β-cell through a "push mechanism" due to substrate pressure enhancing fuel flux, energy production, and extrusion of Na^+ from the cells in contrast to SU receptor (SUR)-1 inhibitors, which may modify intermediary and energy metabolism secondarily through a "pull mechanism" due to higher energy demand resulting from increased ion fluxes and the exocytotic work load. *Diabetes* 52:394–402, 2003

From the [1]Diabetes Research Center and Department of Biochemistry and Biophysics, University of Pennsylvania School of Medicine, Philadelphia, Pennsylvania; the [2]Division of Metabolism, Children's Hospital of Philadelphia, Philadelphia, Pennsylvania; and [3]Pharmacological Research 1, Novo Nordisk, Bagsvaerd, Denmark.

Address correspondence and reprint requests to Nicolai Doliba, D.Sc., University of Pennsylvania, Biochemistry/Biophysics, 501 Stemmler Hall, 36th & Hamilton Walk, Philadelphia, PA 19104. E-mail: nicolai@mail.med.upenn.edu.

Received for publication 5 August 2002 and accepted in revised form 31 October 2002.

R.D.C. holds stock in Novo Nordisk.

GLY, glyburide; IBMX, 3-isobutyl-l-methylxanthine; K_{ATP} channel, ATP-sensitive K^+ channel; LB, line broadening; MDP, methylene diphosphonate; NMR, nuclear magnetic resonance; PCr, P-creatine; PI, phosphatidylinositol; PKC, protein kinase C; SU, sulfonylurea; SUR, SU receptor.

Inhibition of ATP-sensitive K^+ channels (K_{ATP}) by an increase in cytosolic ATP^{4-} or a decrease in $MgADP^-$ and the resultant depolarization are essentially involved in the physiological mechanisms that lead to insulin secretion from pancreatic β-cells (1–5).

The K_{ATP} channel is also the target of hypoglycemic sulfonylurea (SU) drugs, which are of considerable importance for the treatment of type 2 diabetes. Chemically different drugs are currently being investigated, i.e, the classic SU receptor (SUR) drug glyburide (GLY) and the newer drugs repaglinide and nateglinide (6,7). The latter are structurally distinct from traditional SU but show some chemical resemblance to the non-SU moiety of the GLY structure (6). All of these stimulate insulin release from β-cells via inhibition of the K^+ channel, but they differ in their degree of specificity for the pancreatic β-cell SUR subtypes. Native K_{ATP} appear to be a complex of a 140-kDa SUR and an inwardly rectifying K^+ channel serving as a pore-forming subunit (KIR6.2) (8). It has been proposed that insulin-secreting cells are equipped with at least two, and possibly three, distinct binding sites for GLY and repaglinide: one with high affinity for repaglinide (K_D <4 nmol/l) and lower affinity for GLY (K_D 14 nmol/l), a second with a high affinity for GLY (K_D 25 nmol/l) but low affinity for repaglinide (K_D >500 nmol/l), and a third (+)-3-(3-hydroxyphenyl)-*N*-1-pro-pyl)-piperadine (PPP)-sensitive high-affinity (K_D 8 nmol/l) repaglinide and GLY site (6). Although the molecular mechanisms are not fully understood, two signaling pathways seem to be modified by SUs in the β-cell. The first involves the inhibition of K_{ATP}, which causes membrane depolarization, calcium influx, and finally activation of the insulin secretory machinery; and a second one involves protein kinase C (PKC) independently of the K_{ATP} (6). However, it has been shown that the mechanism does not involve a direct activation of the enzyme, although the K_{ATP}-independent stimulation of exocytosis by SUs may require functional PKC (9).

It has also been shown that GLY, having a lipophilic nature, enters pancreatic islets (10,11) and exerts a variety

of intracellular actions. Eighty to ninety percent of the SU binding proteins are associated with intracellular membranes, including those of the secretory granules (12,13). It has become evident that SUs may also promote insulin secretion by direct interaction with the secretory machinery not involving closure of the plasma membrane K_{ATP} (13,14). This effect was dependent on PKC and was observed at therapeutic concentrations of SUs (13). Barg et al. (15) have shown that the effect of SUs on exocytosis in pancreatic β-cells is secondary to their binding to 140-kDa high-affinity SURs in the granular membrane. Their action is mediated by a granular 65-kDa mdr-like protein, which may affect granular Cl^- conductance. There is evidence in the literature that GLY affects respiration and ATP content in rat islets (16–19). Through use of islet homogenates, tolbutamide (another SU) and its analogs have been shown to inhibit islet phosphodiesterase (20) and increase c-AMP levels. SUs also modulate the sodium content in rat pancreatic islets (21,22). The mechanisms by which SUs alter intermediary metabolism can be expected to differ from those that underlie the effects of high glucose. However, previous pharmacological studies have not focused on the contributions of free adenine nucleotide and free Na levels, even though this aspect may be of significance for long-term efficacy. Hypoglycemia could be caused by lowering the threshold for glucose-stimulated insulin release. A more complete understanding of this potential complication is needed in order to better optimize drug therapy.

Therefore, the present study was designed to explore the actions of GLY on the energetics and Na^+ metabolism of β-HC9 cells as they relate to insulin release. To accomplish this we used noninvasive ^{31}P and $^{23}Na^+$-neuclear magnetic resonance (NMR) technology, respirometry, and radioimmunoassays for insulin and c-AMP to compare the effect of high glucose (30 mmol/l) with the effect of GLY in continuously superfused β-HC9 cells complemented by selected studies with isolated β-HC9 cell mitochondria.

RESEARCH DESIGN AND METHODS

General procedures. The β-HC9 cell line was obtained from Dr. D. Hanahan. Cells were maintained in Dulbecco's modified Eagle's medium with 15% FCS and 24 mmol/l glucose. β-HC9 cells of passages 22–28 were used in this study. Cells were supplemented with 25 mmol/l creatine 48 h before the experiment. The cellular protein content was measured by the method of Lowry et al. (23).

Formation of beads. Cells were placed in agarose beads (bead size 800–1,000 μm; 2000–2500 beads/cm^3) to maintain them in a stable environment and prevent them from escaping from the superfusion system (24). Briefly, cells were suspended in 1 ml Krebs-Ringer bicarbonate buffer containing: 114 mmol/l NaCl, 5 mmol/l KCl, 24 mmol/l $NaHCO_3$, 1 mmol/l $MgCl_2 \times 6H_2O$, 25 mmol/l creatine, 2.2 mmol/l $CaCl_2$, 10 mmol/l HEPES (pH 7.4), and 3 mmol/l glucose. Cells suspended in this buffer were then added to 1 ml 6% agarose (Sigma type VII, low gelling temperature) and mixed at 37°C. This suspension was then decanted into 50 ml paraffin oil (37°C) and stirred continuously. The interaction (difference in surface tension) of the oil and agarose caused bead formation. Beads were cooled to 10°C by adding ice to the water bath under continuous stirring for 5 min to allow them to become firm and to maintain their shape. The beads were irregularly shaped with an average size of 1-mm diameter, as was determined by phase contrast microscopy (Nikon TMS). Beads containing cells were suspended in buffer and washed several times.

Preparation of isolated mitochondria. Mitochondria from β-HC9 cells were isolated by differential centrifugation according to the generally accepted scheme with modifications providing protection of their native state (25). Briefly, 1–2 × 10^9 cells were washed twice with a buffer containing 250 mmol/l sucrose, 20 mmol/l HEPES (pH 7.4), 0.5 mmol/l EDTA, and 0.25% BSA and homogenized in the same buffer using a glass Potter-Elvehjem homogenator with a motor-driven Teflon pestle. After initial centrifugation (7 min at 480*g*), the pellet containing nuclei and other cellular debris was discarded. The supernatant was centrifuged at 10,000*g* for 15 min to obtain the mitochondrial fraction.

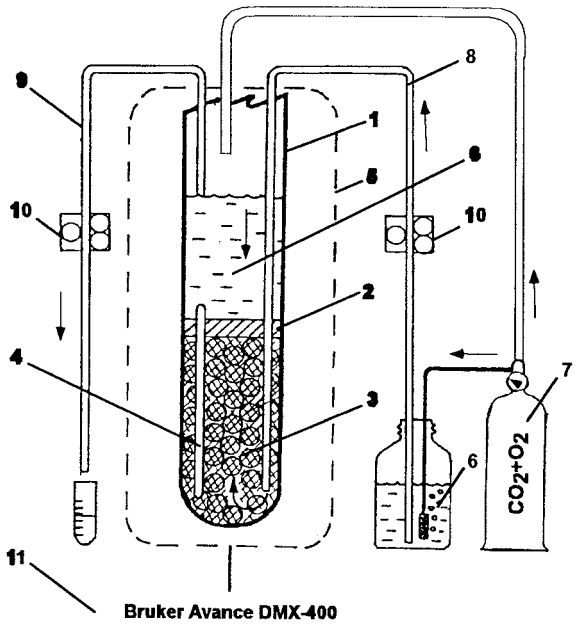

FIG. 1. Scheme of perifusion system for noninvasive cell NMR studies. *1*) glass NMR tube; *2*) filter (100 μm pore size); *3*) agarose beads with cells; *4*) methylene diphosphonate standard; *5*) NMR probe; *6*) superfused buffer (37°C, pH 7.4); *7*) tank with gas mixture (95% O_2 + 5% CO_2); *8*) inflow line (at 2.7 ml/min); *9*) suction line; *10*) pumps; and *11*) spectrometer. Arrows indicate direction of flow.

Perfusion apparatus for oxygen consumption experiments. Beads containing cells were placed between two ~100-μm filters in a flow-through column (Bio Rad). Oxygen partial pressure was recorded polarographically with Clark-type oxygen electrodes placed in inflow and outflow. The superfusion medium was maintained at 37°C using a water bath. The oxygen consumption rate was calculated from the flow rate and the difference in the oxygen partial pressure between the influent and the effluent using the Bunsen absorption coefficient (26). The effluent from the cells was collected for insulin and cAMP measurements. The composition of the perfusion solution was: 114 mmol/l NaCl, 5 mmol/l KCl, 24 mmol/l $NaHCO_3$, 1 mmol/l $MgCl_2 \times 6H_2O$, 25 mmol/l creatine, 2.2 mmol/l $CaCl_2$, 0.1 mmol/l IBMX, and 10 mmol/l HEPES (pH 7.4).

Perfusion apparatus for NMR experiments. Beads containing cells were placed in a 10-mm diameter glass NMR tube and maintained in place by a filter (100 μm pore size) (Fig. 1). Each NMR sample contained ~1.5 ml of beads suspended in 1 ml buffer (20 mg cell protein). The cells and the capillary tube containing methylene diphosphonate (MDP) and NaCl with disprosium standards were placed within the sensitive volume of the NMR coil. The superfusion medium was equilibrated with 95% O_2 and 5% CO_2 and was maintained at 37°C using a water bath. The temperature in the probe was also maintained by the internal variable temperature controller. The transfer lines were insulated. The buffer was introduced through an in-flow line (at 2.7 ml/min). A suction line, placed above the beads, removed the superfusate. The perfusate was not recirculated. The composition of the perfusion solution was the same as for oxygen consumption measurements.

^{31}P NMR methods. The ^{31}P NMR measurements were performed with a Avance DMX-400 spectrometer at 162 MHz. ^{31}P NMR spectra were acquired consecutively in 5-min periods (500 transients) for up to 8 h without proton decoupling (because the resonances are broad and the ^{31}P-^1H-couplings are relatively small [3–12 Hz]). The following conditions were used: pulse width 36°, sweep width 13 kHz, 16 K data points, and repetition time 0.6 s. Free induction decays were processed with a Lorentz-Gauss window function for resolution enhancement (Bruker parameters: line broadening [LB] −8, maximum of the gaussian function [GB] 0.003).

^{23}Na NMR methods. Intracellular Na^+ concentration was determined using thulium-DOTP (3.5 mmol/l) as shift reagent. The following conditions were used: pulse width 90°, sweep width 6.3 kHz, 4 K data points, and repetition time 0.325 s; 3 Hz LB was applied.

Studies with isolated mitochondria. Mitochondrial respiratory function was measured by the polarographic method of Chance and Williams (27) using

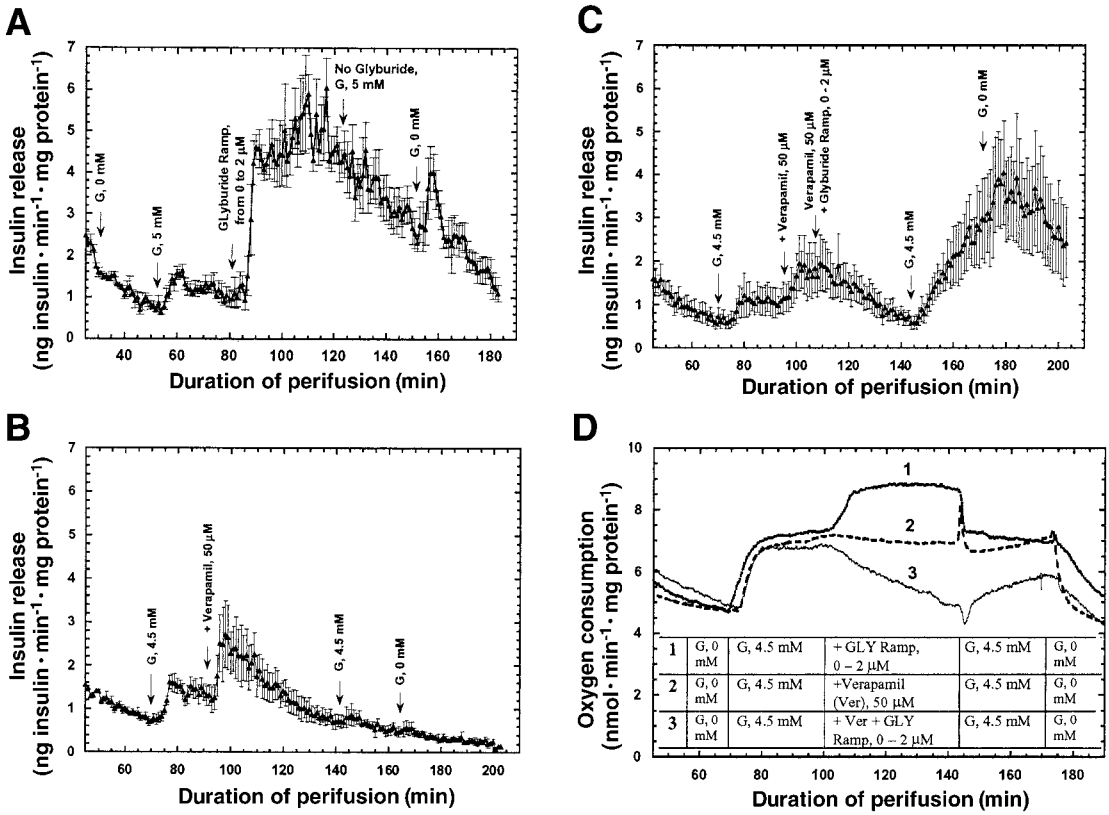

FIG. 2. Enhancement of insulin release and oxygen consumption by GLY. β-HC9 cells embedded in agarose beads were perifused with 5 mmol/l glucose for 30 min and were then exposed to a GLY ramp from 0 to 2 µmol/l using a 50-nmol/l per min increment. *A*) GLY effect on insulin release. *B*) Verapamil effect on insulin release. *C*) Effect of GLY and verapamil on insulin release. *D*) Effect of GLY and verapamil on oxygen consumption. The perifusate also contained 0.1 mmol/l IBMX and 0.5% DMSO as solvent. Each curve represents the mean ± SE of four to five perifusions.

a Clark oxygen electrode. The incubation media contained 250 mmol/l sucrose, 40 mmol/l KCl, 3 mmol/l KH_2PO_4, and 10 mmol/l HEPES buffer (pH 7.4, 27°C). Mitochondrial samples (~1.8–2 mg protein) were added to 1.5 ml incubation media containing succinate (1 mmol/l), pyruvate (0.5 mmol/l) plus malate (0.5 mmol/l), glutamate (2 mmol/l), or glutamine (2 mmol/l) as a substrate for each measurement.

Parameters measured were as follows: state 2, oxygen consumption before the addition of ADP; state 3, oxygen consumption stimulated by ADP (320 nmol); and state 4, oxygen consumption after completion of ADP phosphorylation. The respiratory control index (ratio of state 3 to state 4) was calculated. The ADP-to-O ratio (ratio between the nanomoles of ADP phosphorylated and the nanomoles of oxygen consumed during state 3) was determined and evaluated.

Mitochondrial protein concentration in the polarographic chamber at the end of each experiment was measured by the method of Lowry et al. (23), and results were used to normalize respiratory rates to mitochondrial protein.

Insulin and c-AMP measurments. Insulin content in efflux samples was measured by radioimmunoassay with charcoal separation (28). Rat insulin from Linco Research served as standard, and Miles anti-insulin antibody from ICN was the primary antibody. The c-AMP assay was performed according to the radioimmunoassay method of Albano and Barnes (29) using the Biotrak cAMP[^{125}I] assay system from Amersham Pharmacia Biotech.

Statistical analysis. Insulin and cAMP release, sodium levels, and P-creatine (PCr)–to–inorganic phosphate (P_i) ratios are presented as the mean ± SE of four to five experiments. Oxygen consumption curves are presented as the mean of the four to five experiments without SE due to the high frequency of sampling (1-s interval). In appropriate cases, significant differences between groups were determined by ANOVA with post hoc analysis using Dunnett's multiple comparison test. $P \leq 0.05$ was considered significant.

RESULTS

Oxygen consumption and insulin release of β-HC9 cells stimulated with high glucose or GLY. To assess the effects of GLY on oxygen consumption and insulin release in β-HC9 cells, GLY concentration was increased progressively from 0 to 2 µmol/l using a 50-nmol/l increment per min. GLY at 250–300 nmol/l had a maximal effect on insulin release (Fig. 2*A*) and oxygen consumption (Fig. 2*D*). Verapamil, a Ca^{2+} channel blocker, completely abolished the GLY effect on insulin release (Fig. 2*C*), implying a critical role for voltage-dependent Ca^{2+} channels in the drug's action. Removal of both verapamil and GLY restored insulin release to a rate approximately fourfold higher than without GLY pretreatment (Fig. 2*C*). The latter effect may be related to the continued inhibition of the channel by GLY due to it's tight binding to the SURs. Verapamil alone causes a transient increase in insulin release (Fig. 2*B*) and did not significantly affect oxygen consumption (Fig. 2*D*, *line 2*). Surprisingly, GLY in the presence of verapamil caused a dose-dependent decrease in oxygen consumption (Fig. 2*D*, *line 3*) in contrast to the effect of GLY alone (Fig. 2*D*, *line 1*). These contrasting results may indicate that GLY has dual effects on oxidative metabolism.

In the second set of experiments, we compared the effect of high glucose (30 mmol/l) and high GLY (1 µmol/l) on oxygen consumption and insulin release from perifused β-HC9 cells (Fig. 3*A* and *B*). According to Hu et al. (7), this concentration causes maximum inhibition of K_{ATP} currents in rat β-cells. However, other investigators reported 100% inhibition of K_{ATP} channels at concentrations <100 nmol/l (30). As a functional test of fuel responsiveness, the glucose was removed for 30 min, and then reintroduced at

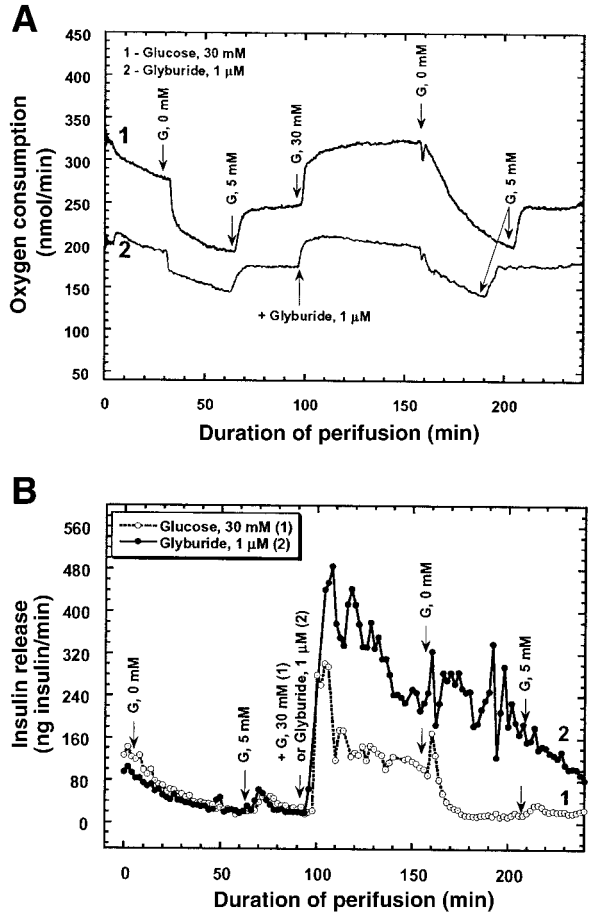

FIG. 3. Effect of GLY on oxygen consumption (*A*) and insulin release (*B*) in β-HC9 cells. β-HC9 cells were preperifused with 5 mmol/l glucose and were then exposed to either 30 mmol/l glucose or 1 μmol/l GLY + 5 mmol/l glucose to assess their effects on insulin release and respiration simultaneously. Cell protein concentrations were 26.0 and 26.6 mg for experiments 1 and 2, respectively. Typical traces of oxygen consumption and insulin release are presented (n = 6).

5 mmol/l for 30 min. Subsequently, cells were exposed to either 30 mmol/l glucose or 1 μmol/l GLY plus 5 mmol/l glucose. Whereas high glucose caused a greater increase in oxygen consumption than GLY (Fig. 3*A*) (30 and 15%, respectively), GLY stimulated insulin release from β-cells to a higher extent than high glucose (Fig. 3*B*) (25- and 15-fold, respectively).

Effect of GLY on ^{31}P-NMR spectra of superfused β-HC9 cells. Figure 4 presents selected ^{31}P-NMR spectra of superfused β-HC9 cells with low (3 or 5 mmol/l) and high (30 mmol/l) glucose and in the presence of 1 μmol/l GLY. Each spectrum clearly displays the resonances of P_i, PCr, and ATP (γ, α, and β) peaks. Results of continuous monitoring (every 5 min) of phosphorus metabolites are presented in Fig. 5*A* and *B*. Increasing the glucose concentration in perfusate from 3 to 30 mmol/l leads to a marked increase in phosphorylation potential, as evidenced by increased PCr and decreased P_i peak areas. The ATP level as indicated by the β-peak of the nucleotide remains constant. In contrast, addition of 1 μmol/l GLY to the cells superfused with 5 mmol/l glucose leads to decreased PCr and increased P_i levels without significant changes in the ATP peaks. GLY decreased the PCr-to-P_i ratio to 58% ($P <$ 0.01) of basal level at 5 mmol/l glucose (Fig. 5*C*). After removal of either secretagogue, the ATP level in glucose pretreated cells remained unchanged in contrast to a decrease in ATP in the cells pretreated with GLY. The PCr decreased and P_i increased in both conditions. The addition of 30 mmol/l glucose restored the phosphorylation potential in both cases.

Effect of GLY on mitochondrial oxidative phosphorylation. To better understand the mechanism of GLY action on ATP production, we extended our study by measuring the respiration and oxidative phosphorylation of mitochondria isolated from β-HC9 cells. Figure 6 presents mitochondrial oxygen consumption data in metabolic states 2, 3, and 4 during oxidation of glutamine (2 mmol/l) (Fig. 6*A*), succinate (1 mmol/l) (Fig. 6*B*), glutamate (2 mmol/l) (Fig. 6*C*), and pyruvate (0.5 mmol/l) plus malate (0.5 mmol/l) (Fig. 6*D*). The addition of 1 μmol/l GLY to mitochondria, oxidizing glutamine or glutamate, completely abolished the stimulation of respiration by ADP (state 3). However, GLY did not affect state 3 respiration when succinate or pyruvate plus malate were

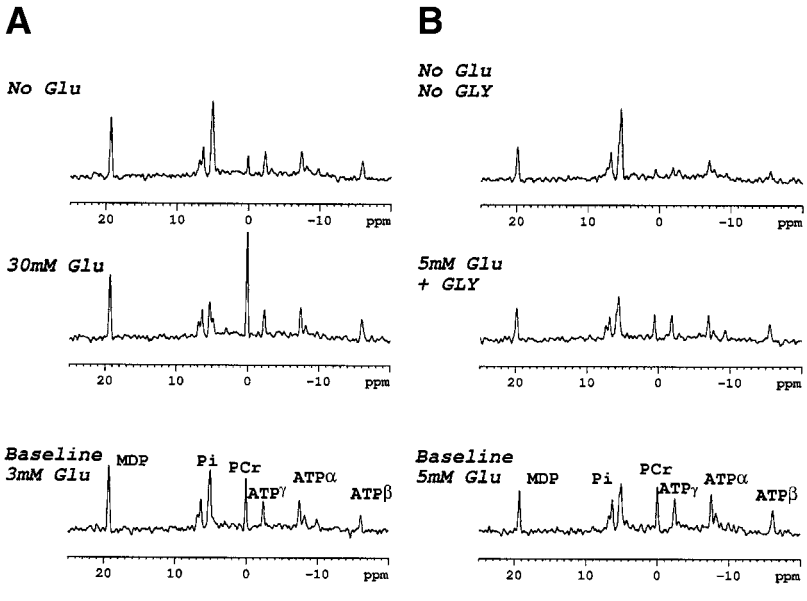

FIG. 4. ^{31}P NMR spectra of superfused β-HC9 cells during baseline glucose concentration (3–5 mmol/l) and during exposure to either 30 mmol/l glucose (*A*) or 1 μmol/l GLY + 5 mmol/l glucose (*B*) followed by washout period. Each exposure lasted 30 min, and each ^{31}P NMR spectrum (acquired in 5-min periods [5,000 transients]) represents the last spectrum of each intervention. Peak assignments are indicated as follows: MDP, methylene diphosphonate standard; P_i, inorganic phosphate; PCr, phosphocreatine; ATP, adenosine triphosphate (γ, α, and β).

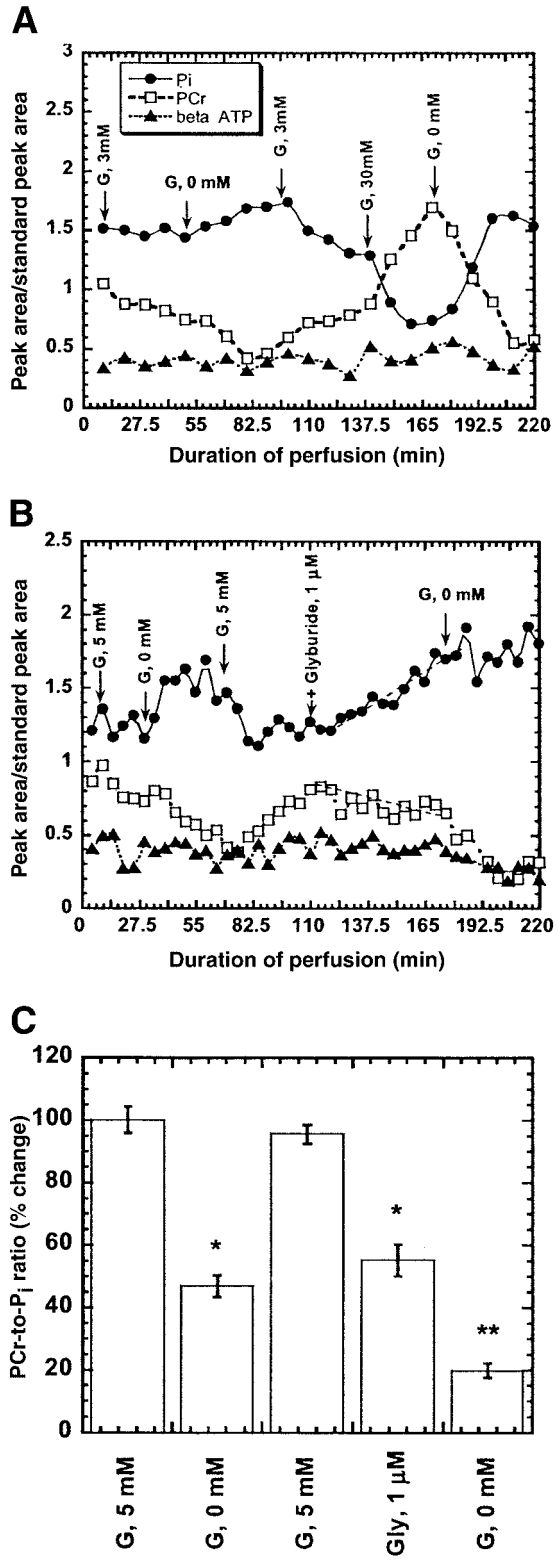

FIG. 5. Effect of high glucose (*A*) and GLY (*B*) on P_i, PCr, and β-ATP of superfused β-HC9 cells. ^{31}P NMR spectra were acquired consecutively in 5-min periods. For clarity, typical experiments are presented (n = 5). *C*: PCr-to-P_i ratio for the experiment in *B*. The ratio (means ± SE) was calculated by averaging the PCr and P_i values for all steady state measurements, and the initial ratio at 5 mmol/l glucose was set to 100%. *$P \leq 0.05$; **$P \leq 0.01$.

used as substrates. The study suggests that GLY selectively affects the oxidation of glutamine and glutamate as evidenced by absence of ADP-stimulated respiration (state 3), meanwhile leaving oxidation of other substrates unchanged.

Effect of GLY on intracellular Na^+ concentration in β-HC9 cells: ^{23}Na-NMR spectroscopy study. The depolarization of the β-cell by GLY causes Ca^{2+} to enter the cell through voltage-dependent calcium channels. An increase in cytosolic-free calcium levels triggers the release of insulin (31–33). The depolarization of the cells may also cause Na^+ to enter the cell. Increased cytosolic sodium may contribute to an increase in cytosolic-free Ca^{2+} via a plasma membrane sodium-calcium exchanger (34). Thus, Na^+ may be an important regulator of calcium metabolism in β-cells. We applied ^{23}Na-NMR spectroscopy to monitor the changes in intracellular Na^+ in β-HC9 cells superfused with either high glucose or GLY. Figure 7 shows the continuous changes in intracellular sodium during perfusion of the cells with different concentrations of glucose and with 1 μmol/l GLY during a representative experiment. Exposure to 5 mmol/l glucose decreased Na^+ to 75% ($P < 0.01$) of basal level; 30 mmol/l glucose resulted in a further decrease in cytosolic Na^+ to 60% ($P < 0.01$) of basal level. In contrast, Na^+ increased to 116% ($P < 0.05$) when 1 μmol/l GLY was added to the perfusate containing 5 mmol/l glucose. Removal of both GLY and glucose caused a further increase of Na^+ up to 140% ($P < 0.01$).

Effect of GLY on cAMP release by β-HC9 cells. Figure 8*A* presents results of the continuous measurement of cAMP release from β-HC9 cells during glucose and GLY-stimulated insulin release. The pattern of cAMP release is similar to changes in insulin release and oxygen consumption in β-HC9. Both high glucose and GLY markedly enhance cAMP release in β-HC9 cells. To evaluate whether the GLY-induced changes in cAMP are related to cellular Ca^{2+} entry, we omitted Ca^{2+} from the perfusion solution containing 5 mmol/l glucose. Thirty minutes later we added 1 μmol/l GLY (Fig. 8*B*). Removal of Ca^{2+} from the perfusion solution initiated the appearance of two discrete spikes in both insulin and cAMP release, which may be due to Ca^{2+} release from intracellular depots. This was then followed by a decrease in insulin secretion, and the further addition of GLY did not stimulate insulin or cAMP release in Ca^{2+}-free solution. However, reintroduction of Ca^{2+} led to a burst of insulin and cAMP release. After removal of GLY from the perfusate, insulin and cAMP release remained elevated, consistent with the tight binding of GLY to the SURs. Uncoupling of respiration and oxidative phosphorylation by FCCP led to decreases in both insulin and cAMP release.

DISCUSSION

Both high glucose and SUs increase oxygen consumption of β-HC9 cells. However, in the case of high glucose, an increase in oxygen consumption is associated with a large increase in the PCr-to-P_i ratio (an indication of a increased P-potential of the β-cells), which is the result of "substrate pressure" and increased production of NADH by glycolysis and Krebs cycle. GLY lowers the PCr-to-P_i ratio, contrasting with the observation after high glucose, while ATP levels in both conditions remain unchanged. The results

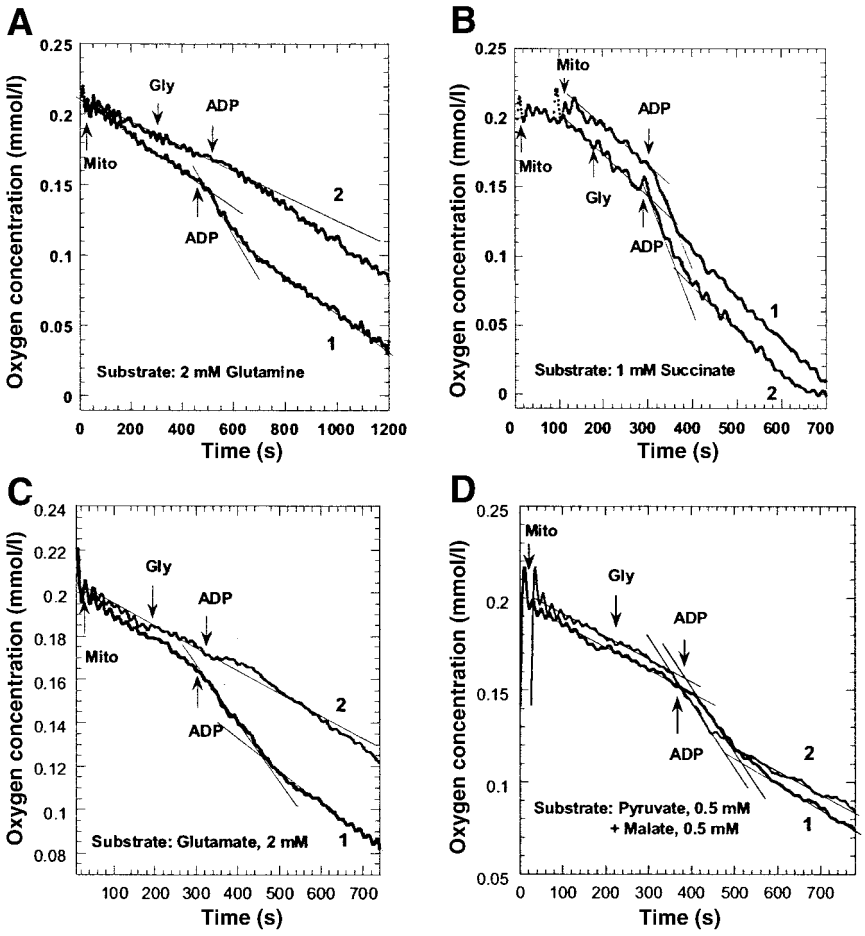

FIG. 6. Effect of GLY on ADP-stimulated oxygen consumption of isolated β-HC9 cell mitochondria during oxidation of glutamine (*A*), succinate (*B*), glutamate (*C*), or pyruvate plus malate (*D*). Figures present a typical (from six to seven experiments) oxygen electrode tracing of mitochondria from β-HC9 cells in the presence (state 3) and absence (state 4) of ADP. State 3 is initiated by addition of ADP (200 μmol/l), and state 4 begins when ADP is consumed. In all panels trace one is substrate alone and trace two is substrate plus 1 μmol/l GLY. Typical experiments are shown (n = 5–6).

suggest that GLY, in contrast to glucose, causes an energy deficit. These data complement recent findings of others (35) who have shown that GLY decreased the islet ATP and ADP content as well as the ATP-to-ADP ratio at 0 mmol/l glucose. However, these effects were no longer observed at 10 mmol/l glucose.

It seems likely that inhibition of K_{ATP} during glucose-stimulated insulin release is due to changes in free ADP concentration (36). The effective level of ATP that inhibits the channel was found to vary in different studies, with half-maximal inhibition occurring at concentrations between 15 and 200 μmol/l (37,38). Because free ATP concentrations in the β-cell are in the millimole per liter range, two explanations have been advanced to explain why K_{ATP}s are not closed at the ambient concentrations of ATP found in the β-cell. ADP^{3-} may compete with ATP for binding to the channels and increases the K_i of ATP, or it may be an activator per se in the form of $MgADP^{-}$. The

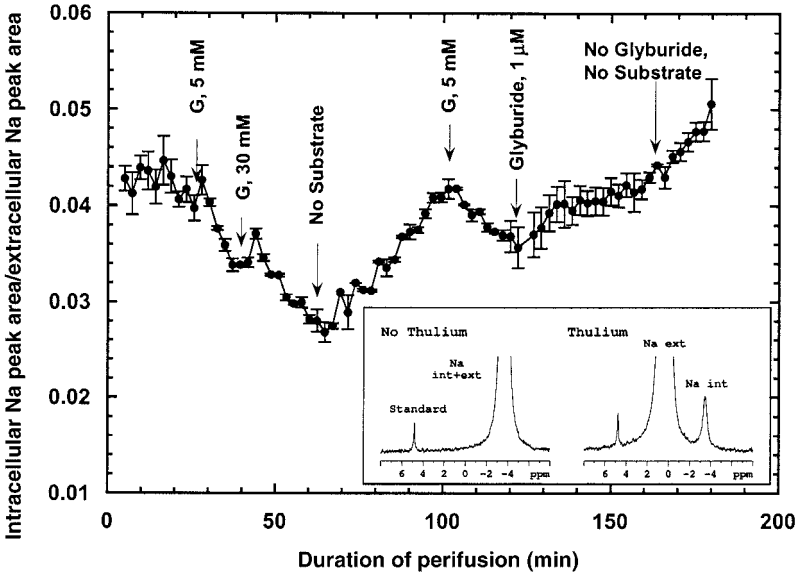

FIG. 7. Effect of GLY on sodium level in superfused β-HC9 cells. Intracellular Na^+ concentration was determined by ^{23}Na NMR using thulium-DOTP (3.5 mmol/l) as shift reagent. Values are mean ± SE; n = 4. Insert shows effect of thulium-DOTP upon ^{23}Na spectra. Addition of thulium-DOTP results in splitting of intra- and extracellular Na signals.

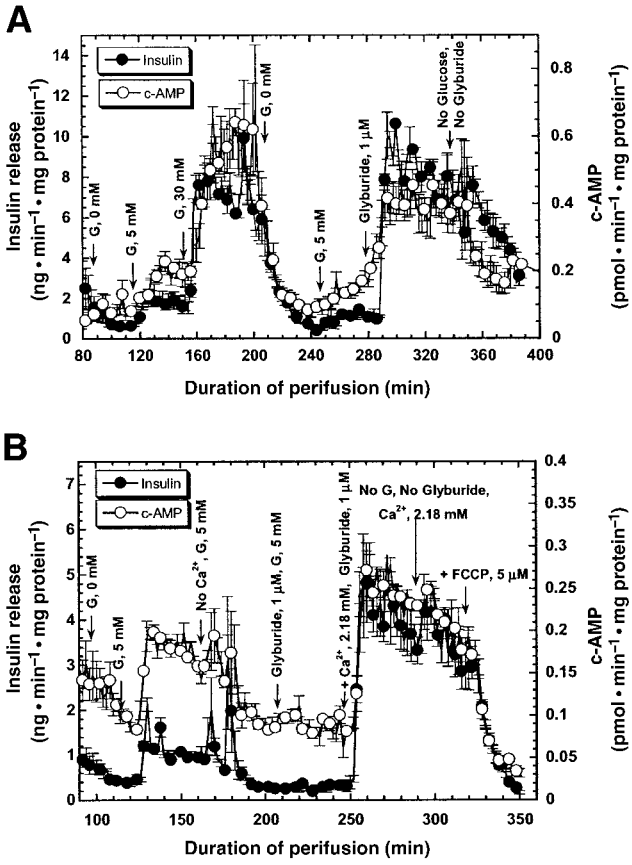

FIG. 8. Insulin and cAMP release of superfused β-HC9 cells. *A*: Glucose and GLY-induced insulin and cAMP release. *B*: Role of calcium in GLY-stimulated insulin and cAMP release. Most curves are the means ± SE of four to five perifusions. The respiratory tracing is a typical example.

latter explanation is more plausible. Thus, ADP may partially reverse the inhibition of the channel by ATP. It has been shown recently that phosphatidylinositol (PI) phospholipids, like $PI(4,5)P_2$, antagonize nucleotide inhibition of K_{ATP} channels, enhancing the coupling of metabolic events to cell electrical or transport activity (39).

GLY appears to stimulate respiration by mechanisms that are distinct from those that underlie the effects of high glucose. Applying digital Ca^{2+} imaging on single β-TC3 cells, it has been shown that repaglinide and GLY induce a concentration-dependent increase in intracellular free Ca^{2+} concentration (40). The increase in $[Ca^{2+}]_i$ results from Ca^{2+} entry through voltage-dependent L-type Ca^{2+} channels because it is inhibited by verapamil. Based on studies of the heart and other tissues, it has been suggested that increases in cytosolic Ca^{2+} concentration may lead to an increase in intramitochondrial free Ca^{2+} and activation of several matrix dehydrogenases and increased turnover of the Krebs cycle (41). However, increased turnover of the Krebs cycle would lead to increased ATP synthesis, which is in contrast to the drop in ATP level seen in the GLY-stimulated β-cells. Panten et al. (42) suggested that the driving force for tolbutamide-induced oxygen uptake is a decrease in the phosphorylation potential caused by the workload imposed by stimulation of the secretion process.

Our experiments with verapamil, a calcium channel blocker, indicate that in addition to having a stimulatory effect on oxygen consumption, GLY may inhibit oxidative metabolism as seen when the voltage-dependent L-type Ca^{2+}-channels are inhibited. To directly explore the mechanisms by which GLY affects oxidative phosphorylation, we studied mitochondria isolated from β-cells. It has been shown that GLY enters the β-cell and is associated with secretory granules and accumulates in concentrations (43) far in excess of those needed to occupy the SURs (44). Mitochondria might thus be a target of SU action. GLY was added to isolated mitochondria oxidizing NAD- and FAD-dependent substrates. Although a high concentration of GLY was used in this study, we found that GLY selectively affects the oxidation of glutamine and glutamate. In contrast, ADP was able to stimulate the oxidation of succinate and pyruvate plus malate in the presence of GLY, which is indicative of a viable state 3 respiration in the mitochondria.

The results also suggest that GLY does not have a direct uncoupling effect on respiration and oxidative phosphorylation (i.e., the P-to-O ratio is not changed during oxidation of pyruvate plus malate or succinate). However, we cannot exclude the possibility that in vivo GLY may be able to induce Ca^{2+} overload in cells and may lead to uncoupling of respiration and oxidative phosphorylation.

It has been demonstrated with the patch clamp technique that pancreatic β-cells are equipped with potential-dependent Na^+ channels (22,45–47) and that glucose promotes Na^+ entry via such channels. This effect was counteracted by both the hyperpolarizing agent diazoxide and the Na^+ channel blocker tetrodotoxin. It also has been shown that exposure of β-cell–rich pancreatic islets from *ob/ob* mice to glucose resulted in a protracted lowering of the sodium content, as measured by integrating flame photometry (48,49). The maximum effect was seen at 5 mmol/l glucose, with no additional reduction when glucose was increased to 20 mmol/l (49). There was no indication that glucose-induced lowering of sodium reflected the activation of the ouabain-sensitive Na/K pump when measuring the uptake of $86Rb^+$ (48). However, other authors (35) demonstrated that D-glucose stimulates the Na^+/K^+ pump and further suggested that this may be part of the membrane repolarization process, following the primary depolarization by these agents. Wesslen and Hellman (1988) (48) suggested that glucose facilitates the removal of Ca^{2+} from cytoplasm by increasing the transmembrane Na^+ gradient (48). The radioisotope studies of Kawazu et al. (50) have shown that glucose stimulates both entry and the extrusion of Na^+ from the β-cells. Because GLY depolarizes the β-cells, it was of interest to evaluate the effect of the drug on Na^+ transport. NMR technology allowed us to continuously monitor the changes in intracellular free Na^+ concentration of perifused agarose embedded β-HC9 cells every 2.3 min. Results of our study show that GLY and high glucose had opposing effects on intracellular Na^+ levels in β-cells. Both low and high glucose lower the Na^+ level in β-HC9 cells, whereas GLY increases the intracellular ion concentration. The effect of GLY is more pronounced in glucose-free solution.

Results of the present study also indicate that both high glucose and GLY elevate cAMP (incidentally, the demonstration of this effect requires the presence of 0.1 mmol/l

IBMX). These effects may be due to elevation of intracellular Ca^{2+}, which leads to activation of adenylcyclase. Our results are in agreement with data showing that glucose, in addition to other agents, stimulates insulin secretion through cAMP–dependent mechanisms (20).

These data support the hypothesis that glucose activates β-cells through a "push mechanism" due to substrate pressure, enhancing fuel flux, energy production, and extrusion of Na^+ from the cells in contrast to SUR-1 inhibitors, which may modify intermediary and energy metabolism secondarily through a "pull mechanism" due to higher energy demand resulting from increased ion fluxes and the exocytotic work load.

ACKNOWLEDGMENTS

This work was supported in part by Grants NIDDK 22122 and 19525, a grant from the American Diabetes Association (to N.M.D.), and a grant in aid from Novo Nordisk.

REFERENCES

1. Tsuura Y, Ishida H, Okamoto Y, Tsuji K, Kurose T, Horie M, Imura H, Okada Y, Seino Y: Impaired glucose sensitivity of ATP-sensitive K^+ channels in pancreatic β-cells in streptozotocin-induced NIDDM rats. *Diabetes* 41:861–865, 1992
2. Cook DL, Hales CN: Inracellular ATP directly blocks K^+ channels in pancreatic B cells. *Nature (Lond)* 311:271–273, 1984
3. Ashcroft F, Harrison DE, Ashcroft SJH: Glucose induces closure of sing potassium channels in rat pancreatic β-cells. *Nature (Lond)* 312:446–448, 1984
4. Misler S, Falke LC, Gillis K, Macdaniel ML: A metabolite-regulated potassium channel in rat pancreatic B cells. *Proc Natl Acad Sci U S A* 83:7119–7123, 1986
5. Rorsman P, Berggren O, Bokvist K, Efendic S: ATP-regulated K^+ channels and diabetes mellitus. *N Physiol Sci* 5:143–147, 1990
6. Fuhlendorff J, Rorsman P, Kofod H, Brand CL, Rolin B, MacKay P, Shymko R, Carr RD: Stimulation of insulin release by repaglinide and glibenclamide involves both common and distrinct processes. *Diabetes* 47:345–351, 1998
7. Hu S, Wang S, Dunning BE: Tissue selectivity of antidiabetic agent nateglinide: study on cardiovascular and β-cell KATP channels. *J Pharmacol Exp Ther* 291:1372–1379, 1999
8. Inagaki N, Gonoi T, Clement JP IV, Namba N, Inazawa J, Gonzalez G, Aguilar-Bryan L, Seino S, Bryan J: Reconstitution of IATP: an inward rectifier subunit plus the sulphonylurea receptor. *Science* 270:1166–1170, 1995
9. Tian YM, Johnson G, Ashcroft SJH: Sulfonylureas enhance exocytosis from pancreatic β-cells by a mechanism that does not involve direct activation of protein kinase C. *Diabetes* 47:1722–1726, 1998
10. Gylfe E, Hellman B, Sehlin J, Taljedal I-B: Interaction of sulfonylureas with the pancreatic β-cells. *Experientia* 40:1126–1134, 1984
11. Marynissen G, Smets G, Kloppel G, Gerlache L, Malaisse WJ: Internalization of glimepiride and glibenclamide in the pancreatic β cell. *Acta Diabetol* 29:113–114, 1992
12. Ozanne SE, Guest PC, Hutton JC, Hales CN: Intrcellular localization and molecular heterogeneity of the sulphonylurea receptor in insulin-secreting cells. *Diabetologia* 38:277–282, 1995
13. Eliasson L, Renstrom E, Ammala C, Berggren P-O, Bertorello AM, Bokvist K, Chibalin A, Deeney JT, Flatt PR, Gabel J, Gromada J, Larsson O, Lindstrom P, Rhodes CJ, Rorsman P: PCK-dependent stimulation of exocytosis by sulfonylureas in pancreatic β cells. *Science* 271:813–815, 1996
14. Ammala C, Bokvist K, Eliasson L, Lindstrom P, Rorsman P: Tolbutamide stimulates exocytosis by direct interaction with the secretory machinery in β-cells (Abstract). *Diabetologia* 36 (Suppl. 1):A60, 1993
15. Barg S, Renstrom E, Berggren PO, Bertorello A, Bokvist K, Braun M, Eliasson L, Holmes WE, Kohler M, Rorsman P, Thevenod F: The stimulatory action of tolbutamide on Ca2+-dependent exocytosis in pancreatic beta cells is mediated by a 65-kDa mdr-like P-glycoprotein. *Proc Natl Acad Sci U S A* 96:5539–5544, 1999
16. Hellman B, Idahl L-A, Danielsson A: Adenosine triphosphate levels of mammalian pancreatic B cells after stimulation with glucose and hypoglycemic sulfonylureas. *Diabetes* 18:509–516, 1969
17. Krzanowski JJ Jr, Fertel R, Matschinsky FM: Energy metabolism in pancreatic islets of rats: studies with tolbutamide and hypoxia. *Diabetes* 20:598–606, 1971
18. Kawazu S, Sener A, Couturier E, Malaisse W: Metabolic, cationic and secretory effects of hypoglycemic sulfonylureas in pancreatic islets. *Naunyn-Schmiedeberg's Archs Pharmac* 312:277–283, 1980
19. Welsh M: The effect of glibenclamide on rat islet radioactive nucleotide efflux, ATP contents and respiratory rates. *Biochem Pharmacol* 32:2903–2908, 1983
20. Charles MA, Lawecki J, Steiner AL, Grodsky GM: Cyclic nucleotides in pancreatic islets: tolbutamide- and arginine-induced insulin release. *Diabetes* 25:256–259, 1976
21. Ali L, Wesslen N, Hellman B: Sulphonamide modulation of sodium content in rat pancreatic islets. *Eur J Pharmacol* 158:257–262, 1988
22. Saha S, Hellman B: Sulfonylureas mimic glucose in stimulating the uptake of Na^+ in pancreatic islets exposed to ouabain. *Eur J Pharmacol* 258:145–149, 1994
23. Lowry OH, Rosebrough NJ, Farr AL, Randall RJ: Protein measurement with Folin reagent. *J Biol Chem* 193:265–275, 1951
24. Doliba NM, Wehrli SL, Babsky AM, Doliba NM, Osbakken MD: Encapsulation and perfusion of mitochondria in agarose beads for functional studies with ^{31}P-NMR spectroscopy: *Magn Reson Med* 39:679–684, 1998
25. Kondrashova MN, Doliba NM: Polarographic observation of substrate-level phosphorylation and its stimulation by acetylcholine. *FEBS Lett* 243:153–155, 1989
26. Umbreit WW, Burris RH, Stauffer JF: *Manometric Techniques*. Minneapolis, MN, Burgess Publishing, 1947
27. Chance B, Williams GR: The respiratory chain and oxidative phosphorylation. *Adv Enzymol* 17:65–134, 1956
28. Herbert V, Lau KS, Gottlieb CW, Bleicher SJ: Coated charcoal immunoassay of insulin. *J Clin Endocrinol Metab* 25:1375–1384, 1965
29. Albano JDM, Barnes GD: Factors affecting the saturation assay of cyclic AMP in biological systems. *Analyt Biochem* 60:130–141, 1974
30. Zunkler BJ, Lenzen S, Manner K, Panten U, Trube G: Concentration-dependent effects of tolbutamide, meglitinide, glipizide, glibenclamide and diazoxide on ATP-regulated K+ currents in pancreatic B-cells. *Naunyn Schmiedebergs Arch Pharmacol* 337:225–230, 1988
31. Malaisse WJ, Herchuelz A, Devis G, Somers G, Boschero AC, Hutton JC, Kawazu S, Sener A, Atwater IJ, Duncan G, Ribalet B, Rojas E: Regulation of calcium fluxes and their regulatory roles in pancreatic islets. *Ann N Y Acad Sci* 307:562–582, 1978
32. Ashcroft FM, Harrison DE, Ashcroft SJ: A potassium channel modulated by glucose metabolism in rat pancreatic beta-cells. *Adv Exp Med Biol* 211:53–62, 1986
33. Boyd AE, Aguilar-Bryan L, Nelson DA: Molecular mechanisms of action of glyburide on the beta cell. *Am J Med* 89 (Suppl. 2A):3S–10S, 1990
34. Cox D, Matlib M: A role for mitochondrial Na^+-Ca^{2+} -exchanger in the regulation of oxidative phosphorylation in isolated heart mitochondria. *J Biol Chem* 268:938–947, 1993
35. Elmi A, Idahl LA, Sehlin J: Relationships between the Na(+)/K(+) pump and ATP and ADP content in mouse pancreatic islets: effects of meglitinide and glibenclamide. *Br J Pharmacol* 131:1700–1706, 2000
36. Ghosh A, Ronner P, Cheong E, Khalid P, Matschinsky FM: The role of ATP and free ADP in metabolic coupling during fuel-stimulated insulin release from islet beta-cells in the isolated perfused rat pancreas. *J Biol Chem* 266:22887–22892, 1991
37. Cook DL, Santin LS, Ashford MLJ, Hales CN: ATP-sensitive K^+ channels in pancreatic β-cell: spare channel hypothesis. *Diabetes* 37:495–498, 1988
38. Hopkins WF, Fatherazi S, Peter-Riesch B, Corkey BE, Cook DL: Two sites for adenine-nucleotide regulation of ATP-sensitive potassium channels in mouse pancreatic beta-cells and HIT cells. *J Membr Biol* 129:287–295, 1992
39. MacGregor GG, Dong K, Vanoye CG, Tang LQ, Giebisch G, Hebert SC: Nucleotides and phospholipids compete for binding to the C terminus of K_{ATP} channels. *Proc Natl Acad Sci U S A* 99:2726–2731, 2002
40. Gromada L, Dissing S, Kofod H, Frokjensen-Jensen J: Effects of the hypoglycaemic drugs repaglinide and glibenclamide on ATP-sensitive potassium-channels and cytosolic calcium levels in βTC3 cell and rat pancreatic beta cells. *Diabetologia* 38:1025–1032, 1995
41. McCormack JG, Halestrap AP, Denton RM: Role of calcium ions in regulation of mammalian intramitochondrial metabolism. *Physiol Rev* 70:391–425, 1990
42. Panten U, Zunkler BJ, Scheit S, Kirchhoff K, Lenzen S: Regulation of energy metabolism in pancreatic islets by glucose and tolbutamide. *Diabetologia* 29:648–654, 1986
43. Carpentier JL, Sawano F, Ravazzola M, Malaisse W: Internalization of ^{3}H-glibenclamide in pancreatic Let cell. *Diabetologia* 29:259–261, 1986
44. Findlay I: Inhibition of ATP-sensitive K^+ channels in cardiac muscle by the sulphonylurea drug glibenclamide. *J Pharmacol Exp Ther* 261:540–545, 1992

45. Hiriart M, Matteson DR: Na channels and two types of Ca channels in rat pancreatic β-cells identified with the reverse hemolytic plaque assay. *J Gen Physiol* 67:617, 1988
46. Plant TD: Na^+ currents in cultured mouse pancreatic β-cells. *Pflug Arch* 411:429–435, 1988
47. Pressel DM, Misler S: Sodium channels contribute to action potential generation in canine and human pancreatic islet β cells. *J Membr Biol* 116:273, 1990
48. Wesslen N, Hellman B: Characterization of the glucose-induced lowering of sodium in mouse pancreatic β-cells. *Acta Physiol Scand* 133:11–17, 1988
49. Wesslen N, Bergsten P, Hellman B: Glucose-induced reduction of the sodium content in beta-cell-rich pancreatic islets. *Biocience Reports* 6:967–972, 1986
50. Kawazu S, Boschero AC, Delcroix C, Malaisse WJ: The stimulus-secretion coupling of glucose-induced insulin release. XXVIII. Effect of glucose on Na^+ fluxes in isolated islets. *Plugers Arch* 375:197–206, 1978